FORSCHUNGSZENTRUM
ROSSENDORF e.V.

FZR

FZR-58
Oktober 1994
Preprint

S. Frauendorf, S. Reimann and V.V. Pashkevich

Three Contributions to the Seventh International Symposium on Small Particles and Inorganic Clusters

To be published in proceedings of ISSPIC 7,
September 12-16, 1994, Kobe, Japan
Surface Letter and Reviews (World Scientific Pub.)

"Magnetic properties of Sodium Clusters"
registered as JINR preprint E4-94-421

"Shapes and Free Energies of Molten Sodium Clusters"
registered as JINR preprint E4-94-422

Forschungszentrum Rossendorf e.V.
Postfach 51 01 19 · D-01314 Dresden
Bundesrepublik Deutschland

Telefon (0351) 591 3261
Telefax (0351) 591 3700
E-Mail frauendorf@gamma.fz-rossendorf.de

Shapes and Free Energies of Molten Sodium Clusters

S. Frauendorf[1] and V.V.Pashkevich[2]

[1] *Institute for Nuclear and Hadronic Physics, Research Center Rossendorf Inc., PB 51 01 19, D-01314 Dresden, Germany*

[2] *Laboratory for Theoretical Physics, Joint Institute for Nuclear Research, 141980 Dubna, Russian Federation*

The shell correction method is formulated to calculate the shapes and free energies of hot alkali clusters. The equilibrium shapes of Na clusters with mass 50 to 700 are calculated by minimizing simultanously with respect to two deformation parameters. For $T = 700°K$ strong deviations from spheroidal shape including reflection asymmetric shapes are found to survive in the center of the open shells. The second derivative of calculated free energy correlates with the derivative of the experimental cluster abundances, showing prominent spikes related to the change between spherical and deformed shape.

PACS numbers :36.40-32.Bv-

The shell correction method (SCM) developed in nuclear physics has turned out to be an efficient theory to calculate the deformation energy of alkali clusters [1–5]. All these calculations assume zero temperature for the valence electron system, whereas in experiment clusters are formed at several 100 °K. We generalize the SCM to finite temperatures by writing the total free energy of the cluster as the sum of a liquid drop part F_{LD} and a shell correction

$$F = F_{LD} + \delta F \tag{1}$$

Here, F_{LD} is the free energy of a classical drop of neutral liquid Na consisting of N atoms.

$$F_{LD} = fN + 4\pi r_S^2 N^{2/3} \sigma S(\alpha_\mu)/S_0. \tag{2}$$

This expression is justified for molten clusters, which are produced in smoke sources. It will not be suited for cold clusters when the ions tend to arrange into geometrical structures [9]. For a typical temperature of $T = 600°$K one has $f = -1.427$ eV, $r_S = 2.19\mathring{A}$ and $\sigma = 0.0105eV/\mathring{A}^2$, which are, respectively, the bulk values of free energy per atom, the Wigner - Seitz radius and surface tension, as given in ref. [10,11]. The surface area $S(\alpha, \alpha_3, \alpha_4)$ depends on the deformation parameters $\alpha, \alpha_3, \alpha_4$, which fix the quadrupole, octupole and hexadecapole moments, respectively [1].

The term $\delta F$is the shell correction. It is the difference between the the free energy F_V of the valence electrons in the average potential U generated by them and the ions and the free energy $\tilde{F}_V$ of the "unquantized" valence electrons in the same potential.

$$\delta F = F_V - \tilde{F}_V \tag{3}$$

The energies e_i of the valence electrons are calculated for the Woods Saxon Potential

$$h = \frac{\vec{p}^2}{2m} + U_o[1 + exp(l(\vec{x})/d)]^{-1} \tag{4}$$

where $l(\vec{x})$ measures the distance of the point $\vec{x}$ from the surface $U(\vec{x}) = 1/2U_o$. The shape of this equipotential surface is the same as the one used to calculate the surface area $S(N, \alpha, \alpha_3, \alpha_4)$ in the liquid drop part. The volume of the equipotential surface is kept constant to

$$V_p = N\frac{4\pi}{3}r_P^3, \quad r_P = 2.25\mathring{A} \tag{5}$$

The diffuseness of surface is chosen to be $d = 0.74\mathring{A}$ and U_o=-6eV is the depth of the well (for details c. f. ref. [1]).

The calculation of the free energy is based on the *canonical* ensemble of the valence electrons. This is important, since typical experiments study mass selected cluster beams. The free energy of N independent electrons is calculated as

$$F_V = \lambda N - Tln[\frac{1}{L}\sum_{l=1}^{L} e^{i\frac{2\pi lN}{L}} \prod_j [1 + e^{-\frac{e_j-\lambda}{T} - i\frac{2\pi l}{L}}] \tag{6}$$

For $L \to \infty$ this is the exact expression. [2] We find that $L = 16$ gives the canonical free energy with an relative accuracy better than 10^{-3}, provided λ is chosen such that the mean value of the particle number in the corresponding grand canonical ensemble is equal to N. Our method to evaluate the canonical partition function is different from the one suggested by Brack et al. [8]. It seems to be numerically faster. The accuracy can be controlled by changing L.

The smooth free energy $\tilde{F}_V$ is calculated in the same way as F_V from a set non bunched levels $\tilde{e}_i$. This smooth spectrum is constructed by integrating numerically the smooth level density $\tilde{g}(e)$, calculated by means of the Strutinsky averaging procedure from the spectrum e_i (for the accurate definition of $\tilde{g}(e)$, c. f. ref. [1]).

[1] This is correct for not too large deformation. The accurate definition of the deformation parameters can be found in ref. [1].

[2] This can be seen best by using the projected statistics representation of refs. [6,7].

We have minimized the free energy simultanously with respect to α, α_4 for all even Na clusters in the mass range $50 \leq N \leq 310$ and for the pairs α, α_4 and α, α_3 in the mass range $310 \leq N \leq 730$. Three different temperatures, $T = 0, 0.04$ and 0.06 eV , i.e $0, 465$ and $697°K$ have been studied. The deformation parameters of the average equilibrium shapes are shown in figs. 1 and 2.

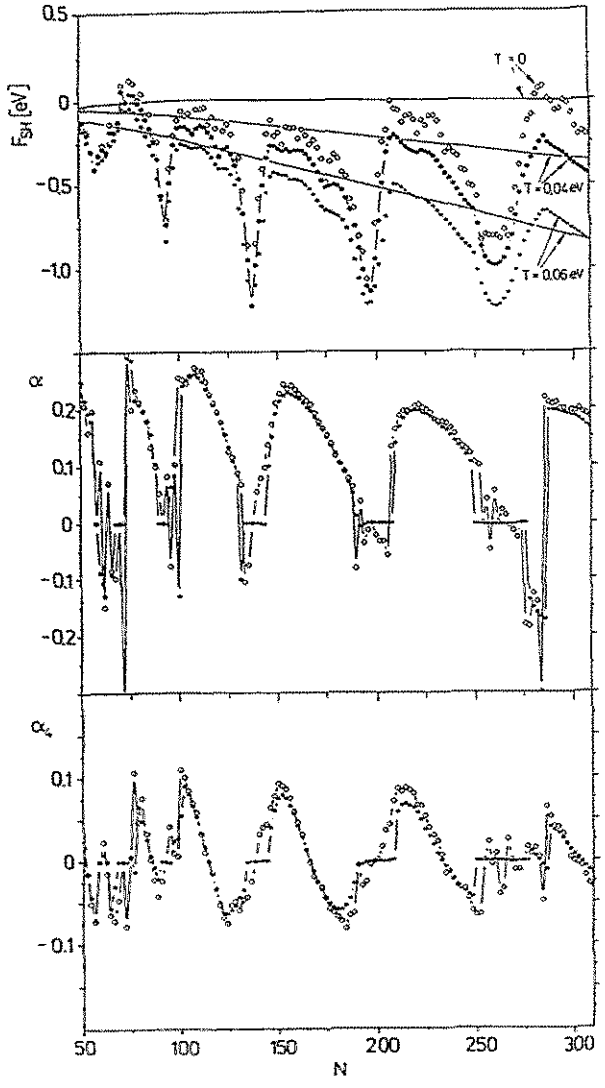

FIG. 1. Shell contribution F_{SH} to the free energy and the deformation parameters α and α_4 of molten Na - clusters. The deformation parameters are shown only for $T = 0$ (diamonds) and $T = 0.06$ eV (stars). The full drawn lines are the the zero lines for F_{SH}.

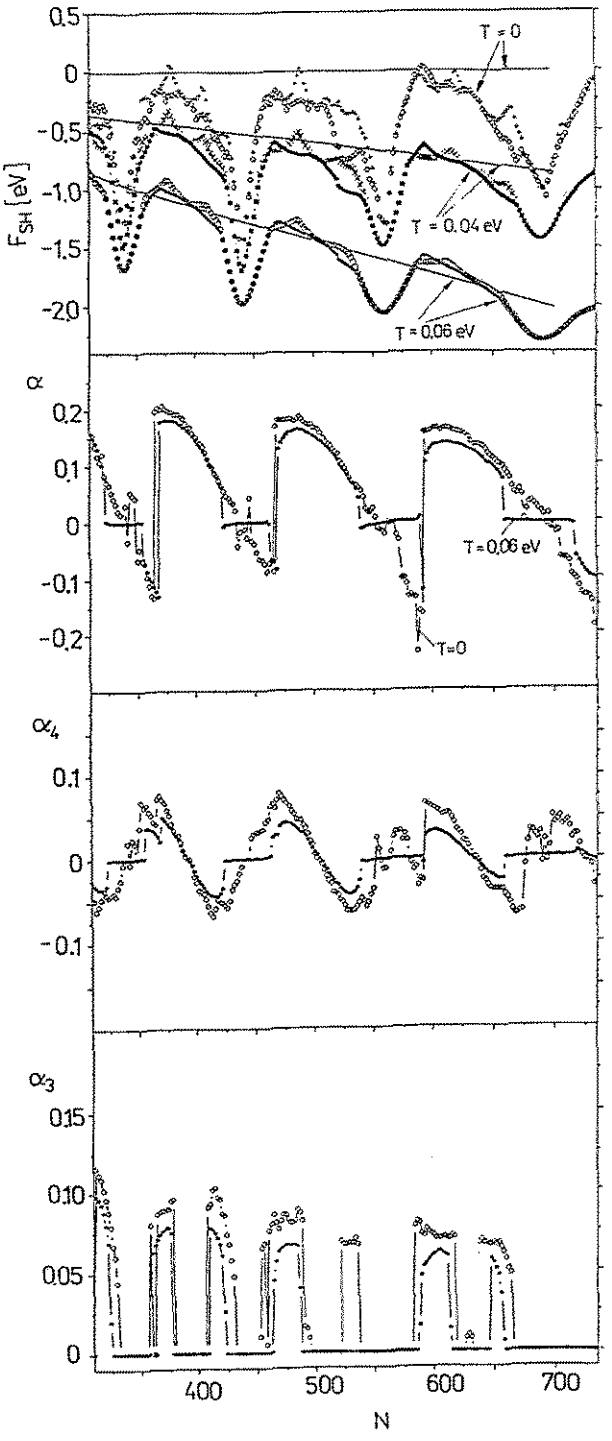

FIG. 2. Shell contribution F_{SH} to the free energy and the deformation parameters α, α_3 and α_4 of molten Na - clusters. The deformation parameters are shown only for $T = 0$ (diamonds) and $T = 0.06$ eV (stars). The full drawn lines are the the zero lines for F_{SH}.

We also display in figures 1 and 2 the shell contribution to the free energy F_{SH}, which is defined as as the free energy at the minimum relative to the free energy of the spherical drop:

$$F_{SH} = F - F_{LD}(sphere) \tag{7}$$

Note, in the figures the zero line of F_{SH} is not horizontal!

The thermal fluctuations tend to wash out the shell structure. The difference between the calculations at $T = 0$ and $T = 700°K$ increases with the mass number N. This is expected, because the the parameter controlling the supression of the shell structure is the ratio $T/\hbar\omega$, where $\hbar\omega \sim 4eVN^{-1/3}$ is the spacing of the shells. Thus, a temperature of $700°K$ is rather low for $N < 50$. In good approximation the valence electron system can be considered as being at zero temperature. For $N > 300$ the same temperature causes a significant suppression of the shell structure.

As cluster deformation is a consequence of the shell structure, it also is suppressed by the thermal fluctuations. Figures 1 and 2 demonstrate that this does not occur as a general decrease of the magnitude of the deformation in the first place. Rather, the regions of sherical shape around the magic numbers are expanding with T and N. It is also seen that the role of the higher multipoles (α_3 and α_4) remains as important as for zero temperature, i. e. the average shapes are about the same as for $T = 0$, provided the cluster is not spherical. One may say that "parts of the deformed regions are melt away". Nevertheless, even for $N \approx 600$ and $T = 700°K$ substantial islands of deformation are left in the center of the open shells.

Such a behavior is a consequence of the fact that the surface $F_{SH}(\alpha, \alpha_3, \alpha_4, T)$ is similar to the $T = 0$ surface $E_{SH}(\alpha, \alpha_3, \alpha_4)$. Only the scale of the relief is reduced and it is smoothed. The deformed minima of the clusters near the magic N are relatively shallow. They become at finite T so shallow that they can no longer compete with the practically T– independent term F_{LD}, which drives towards spherical shape. On the other hand, in the center of the open shells the minima of E_{SH} are deep enough that the reduction of their depth is not large enough to make F_{LD} competativ. They will appear in the total F surfaces at only slightly reduced deformation.

The deformations shown in figures 1 and 2 represent the *average* shape of the ensemble. There are thermal fluctuations around them. The amplitude of these fluctuation is

$$\Delta\alpha \sim \sqrt{T(d^2F/d\alpha^2)^{-1}} \tag{8}$$

In the centers of the spherical and of the deformed regions the term F_{SH} reduces the thermal fluctuations. In the transitional regions, where the deformation melts, the contribution of $d^2F_{SH}/d\alpha^2$ to the total value of $d^2F/d\alpha^2$ is small. There, the thermal fluctuations are much larger, of the order of the fluctuations of the classical drop.

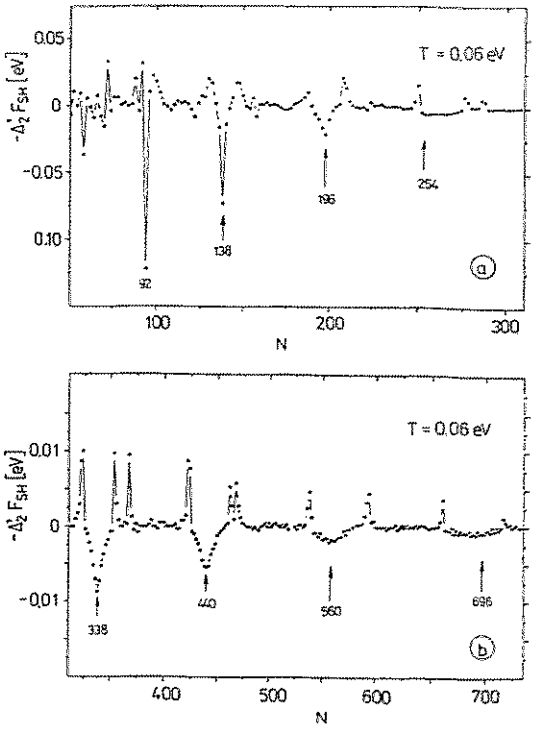

FIG. 3. Second differences of the free energy

Fig. 3 shows the negative second differences of the free energy

$$\Delta_2 F(N) = \frac{1}{4}(+F(N-2) - 2F(N) + F(N+2)) \tag{9}$$

calculated from the equilibrium values of $F(N)$. The negative spikes correspond to the magic numbers, where $F_{SH}(N)$ has a large positive curvature. The shell closure at $N = 254$ is not clean. This is a particular feature of the Woods Saxon potential that shifts the the 3f - level into the shell gap. As a consequence the negative spike is washed out at the considered temperature. The positive spikes appear at beginning and the end of the regions of deformed clusters. If one does not allow for deformation between two magic numbers, the function $F_{SH}(N)$ has the shape of an inverted parabola (c. f. ref. [8]). As seen in figs. 1 and 2, the deformation cuts away the upper part of the parabolas rather sharply, leading to the high curvature at the intersection points that shows up as the positive spikes in fig. 3. The behavior reminds of a second order phase transition. For small systems, as the considered clusters, one must take into account the fluctuations around the average shape in calculating $\Delta_2 F(N)$. These would tend to smooth out the transition, resulting in broader bumps instead of sharp spikes. Our

negative spikes correlate very well with the calculation of $\Delta_2 F(N)$ in ref. [8]. The positive spikes are absent there, since only sherical shapes are studied.

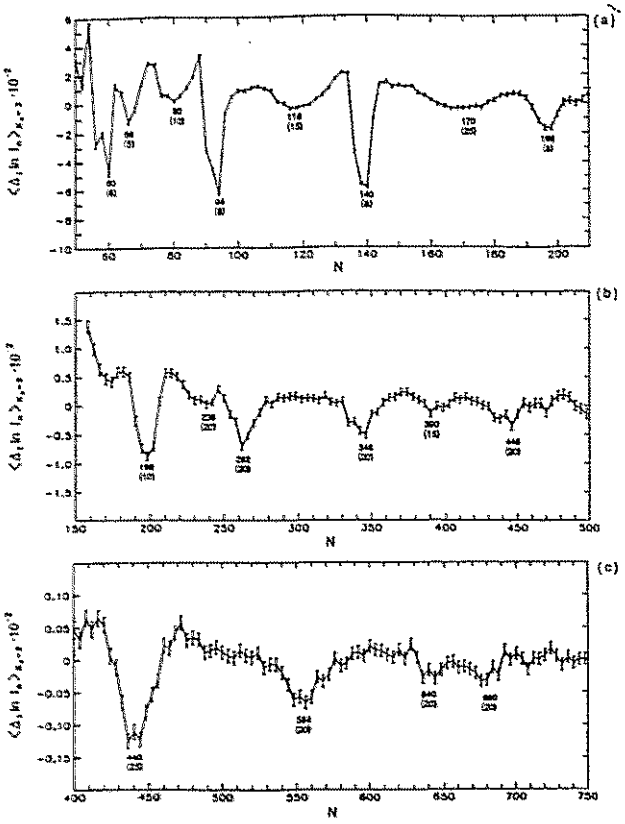

FIG. 4. The first difference of the logarithm of the experimental cluster abundances I as calculated in ref. [5] from the measurments of ref. [12].

For a quantitative comparison of the calculated free separation energies and the experimental abundances one needs a theoretical model for the evaporation cascade. Such work is in progress [13]. Here, we only point out that the shell structure seen in the second differences of the free energies seems to correlate rather well with the shell structure seen in the first differences of the logarithm of the abundances. Not ony the negative spikes caused by the closed shells appear at the the predicted atom numbers, but also the positive spikes cause by the deformation jumps seem to correlate with peaks of the function $\Delta_1 ln(I)$, which are visible up to $N = 300$.

In summary, we have generalized the shell correction approach to finite temperatures. A new renormalization procedure basing on the canonical ensemble has been suggested. For the clusters lying in the center of the open shells the deformation survives thermal fluctuations corresponding to temperatures of hot clusters forming the beam. The higher multipoles of the sphape remain a important as for zero temperature. The regions of spherical shape around the magic numbers expand with increasing temperature and mass number. The onset and the disappearance of deformation seems to show up in the abundancy distribution.

[1] S. Frauendorf, V.V. Pashkevich, Z. Phys D26 (1993) S 98; Phys. Rev. B, subm.

[2] H. Koizuma, S. Sugano, Y. Ishi, Z. Phys. D28 (1993) 223

[3] A. Bulgac, C. Lewenkopf, Phys. Rev. Lett. 71 (1993) 4130

[4] C. Yannouleas, Uzi Landman, Chem. Phys. Lett. 210 (1993) 437; Phys. Rev. B 48 (1993) 8376

[5] S.M. Reimann et al. Z. Phys. D28 (1993) 235

[6] C. Essebag, J. L. Egido, Nucl. Phys. A 552 (1993) 205

[7] R. Rossignioli et al. , Phys. Lett B297 (1992) 9

[8] M. Brack et al., Z. Phys. D21 (1991) 65

[9] T. P. Martin et al., Chem. Phys. Lett. 172 (1990) 209, Z. Phys. D19 (1991) 25

[10] Landolt-Börnstein, *Zahlenwerte und Funktionen aus Physik, Chemie, Astronomie, Geophysik und Technik*, (Springer-Verlag) V IV/2, p.250 ff.

[11] O. Knacke, O. Kubaschewski, K. Hesselmann, *Thermochemical Properties of Inorganic Substances II*, Springer 1991, p. 1314

[12] S. Bjørnholm et al. Phys. Rv. Lett. 65 (1990) 1627

[13] K.Hansen, M Manninen, J. Chem. Phys., subm.; K. Hansen, U. Näher, in preparation

Magnetic Properties of Sodium Clusters

S. Frauendorf[1], V.V.Pashkevich[2] and S. M. Reimann[3]
[1] *Institute for Nuclear and Hadronic Physics, Research Center Rossendorf Inc., PB 51 01 19, D-01314 Dresden, Germany*
[2] *Laboratory for Theoretical Physics, Joint Institute for Nuclear Research, 141980 Dubna, Russian Federation*
[3] *Institute for Theoretical Physics, University Regensburg, D-93040 Regensburg, Germany*

Axial and triaxial shapes of Na clusters are determined by means of the shell correction method [1]. The orbital paramagnetism and the diamagnetism of small Na clusters is calculated. Odd axial clusters may have substantial orbital paramagnetic moments, which are quenched for triaxial shapes. Even clusters show diamagnetism, which is maximal for spherical and attenuated for deformed shape.

PACS numbers :36.40-32.Bv-

It has been demonstrated by de Heer that it is possible to measure the magnetic moments of the lightest Na clusters ($N < 10$) by deflection of the cluster beam in a Stern Gerlach magnet with a field strength of $1T$ [2]. The deflection x is given by

$$x = c\frac{\mu}{NMv^2}\frac{d\omega}{dx} \tag{1}$$

where c is an apparatus constant, N the number of atoms, M the atom mass and v the beam velocity. The magnetic moment μ is measured in units of the Bohr magneton

$$\mu_B = \frac{e\hbar}{2mc} = 0.579 \times 10^{-4} eV/T \tag{2}$$

and the magnetic field B is given as the cyclotron frequency

$$\hbar\omega = \mu_B B \tag{3}$$

For $B = 1T$ one has $\hbar\omega \approx 0.5 \times 10^{-4} eV$. In de Heer's experiments the ratio μ/N that determines the deflection of a cluster is about 0.1.

The response of the electrons to the magnetic field is described by the Hamiltonian [3]

$$H' = H + \omega(l_x + 2s_x) + \frac{\omega^2}{2}(y^2 + z^2) \tag{4}$$

where H is the Hamiltonian at zero field and the direction of the local field defines the x - axis. For $N < 1000$ the spacings between the electron levels are large enough, such that the magnetic field can be treated as a small time independent perturbation. The magnetism of clusters is similar to the one of molecules. The magnetic moment consists of a paramagnetic (0th order) and a diamagnetic (1st order) term.

$$\vec{\mu} = \vec{\mu}_{PAR} + \vec{\mu}_{DIA} \tag{5}$$

I. PARAMAGNETISM

We decompose the the magnetic moment $\vec{\mu}$ with respect to the principal axes 1, 2, 3 of the cluster. The *orbital* paramagnetic moment for the axis i is

$$\mu_i = -(|l_i|) \tag{6}$$

where $|)$ is the ground state of the valence electron system. If i is a symmetry axis, the orbital angular momentum projection Λ is a good quantum number. It gives the orbital paramagnetic moment. The projection Λ takes integer values between 0 and n, the shell number. If the spin orbit coupling is neglected, the levels with $\Lambda = 0$ are twofold degenerate (spin up and down) and the levels with $\Lambda \neq 0$ fourfold (sign of Λ). For the harmonic oscillator $n \approx (N/3)^{1/3}$, leading to a deflection ratio of

$$\frac{\mu}{N} \sim 1 \times N^{-2/3} \tag{7}$$

The measured deflection profile, $I(x)$ is obtained by averaging over all cluster orientations with equal probability. Since there is only one symmetry axis in an axial cluster, the width of the distribution will be reduced by 1/3. Thus, effective deflection parameters of 0.1 and 0.01 are expected for $N = 10$ and 100, respectively. Such values should be detectable with an apparatus like the one used by de Heer.

The orbital paramagnetism appears in odd axial clusters. Since the degeneracy of the $\Lambda \neq 0$ levels is 4, the magnetic moment is equal to Λ of the last valence electron. Fig. 1 shows the orbital paramagnetic moments calculated for odd Na clusters under the assumption that the cluster is axial. The shapes are determined by means of the shell correction method using a Woods Saxon potential (WS) for the valence electrons (c. f. below). Fig. 2 shows a similar calculation based on a somewhat different potential, which we call Kohn Sham Nilsson (KSN). Here we also allow for triaxial deformations. The values of the triaxiality parameter γ are given in the lower panel.

Comparing the axial values of the two figures one notes that the exact cluster numbers N, where the odd electron takes a certain value of Λ, are different, though the general trend is similar. Slight differences in the valence electron potential leads to some reordering of the levels near the Fermi surface, in particular for the heavier clusters. Thus, measurements of the orbital paramagnetic moments could provide information about the finer

details of the deformed valence electron potential. Comparison with the measured magnetic moments is used to fine tune the deformed potential of nuclei.

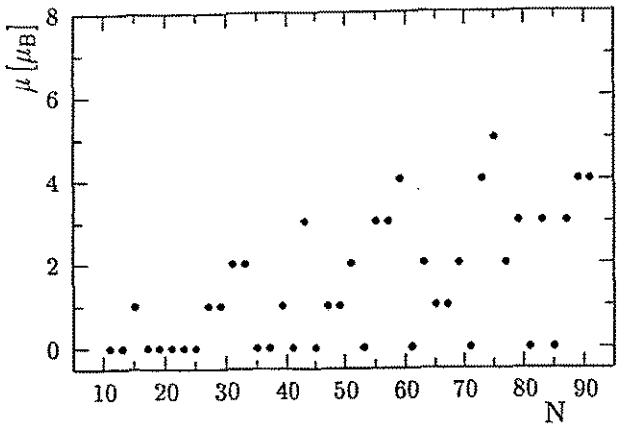

FIG. 1. The orbital magnetic moments of odd Na clusters calculated for the *axial* Woods Saxon potential.

As seen in fig.2, for an appreciable number of clusters the axial shape is not stable. There is a lower triaxial minimum. For these cases we find that $\langle l_i \rangle = 0$ for all three axes, i. e. the orbital paramagnetism is quenched. The quenching of the orbital paramagnetic moment in a nonaxial crystal field is a well known phenomenon in solid state physics [3]. There is also a number of clusters with stable axial shape and strong orbital paramagnetism predicted. Thus, the orbital paramagnetism could serve as a sensitive probe for the deviation of the cluster shape from axiality. It should be noted that we consider only ellipsoidal like shapes. There is also the possibility of nonaxial shapes of higher multipolarity. Their effectiveness in quenching the orbital paramagnetism remains to be studied. It is also necessary to investigate the consequences of the potentials generated by the discrete ions, which are expected to attenuate the magnetic moments.

The electron levels are quasi degenerate with respect to the spin. In odd clusters the all the spins of the electrons are paired off, except the one of the odd electron on the Fermi level. In addition to the orbital part it also generates spin paramagnetism in odd clusters. The interaction with magnetic field will tend to align the spin with direction of the field, but the spin orbit coupling will tend to lock the spin direction to the body fixed frame of the cluster. The clusters in the beam have a thermal rotational energy. This rotation generates a Coriolis force that tends to align the spin with the axis of rotation of the cluster. The angular velocity of the thermal rotation is of the order of the cyclotron frequency, i. e.

$$\hbar\omega \sim \hbar\omega_{ROT} \sim 10^{-4} eV \qquad (8)$$

($T = 500°K$, $N = 100$). Hence the Coriolis force and the torque of the magnetic field are of the comparable. A deeper analysis of this interplay goes beyond the scope of this study, but potentially it contains interesting information on the spin orbit interaction. A thorough study for the trimer has been carried out by de Heer [2]. Experimentally, the spin effects should be best studied for clusters with no orbital paramagnetism.

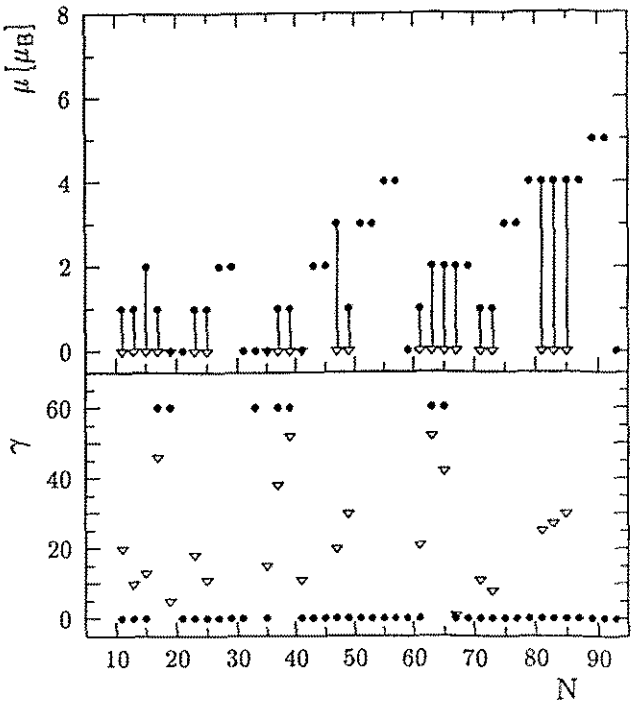

FIG. 2. The orbital magnetic moments of odd Na clusters calculated for the Kohn Sham Nilsson potential. Dots display the lowest axial minima and triangles triaxial minima. The quenching of the orbital magnetic moment by triaxial deformation is demonstrated by the vertical lines. The lower panel shows the triaxiality parameter γ.

In even triaxial clusters the orbital angular momentum is quenched and the spins are paired off, since the electron levels are only twofold degenerate (Kramers degeneracy). Such clusters do not show paramagnetism. In even axial clusters two possibilities exist: If the Fermi level has $\Lambda = 0$ the spins are paired off and there is no paramagnetism. If the Fermi level has $\Lambda \neq 0$ there is the question of how the two electrons occupy the 4 quasidegenerate levels. Most likely, they will follow Hund's rule, i. e. the two spins will align. Then there is no orbital paramagnetic moment and the coupling of the spin is governed by the same interactions as mentioned above for the spin of the odd particle.

II. DIAMAGNETISM

The first order term for the component i of the magnetic moment is

$$\mu_i = -(N\Theta_I + \Theta_i - \mathcal{J}_i)\omega_i \tag{9}$$

It consists of the three contributions:
1) The magnetic susceptibility of the Na ions

$$N\Theta_I = (Z-1)\frac{2}{5}mr_I^2 N \sim 0.51 N\hbar^2 eV^{-1} \tag{10}$$

2) The valence electron diamagnetic susceptibility

$$\Theta_i = m\int \rho(\vec{x})(x_{i+1}^2 + x_{i+2}^2)d^3x \sim 0.26 N^{5/3}\hbar^2 eV^{-1} \tag{11}$$

where $\rho(\vec{x})$ is the electron density
3) The van Vleck term

$$\mathcal{J}_i = \sum_n \frac{|\langle n|l_i + 2s_i|0\rangle|^2}{E_n - E_o} \tag{12}$$

where $|0\rangle$ and $|n\rangle$ are the ground and excited (particle - hole) states of the electron system. The term is zero for a symmetry axis else it is positive, i. e. paramagnetic.

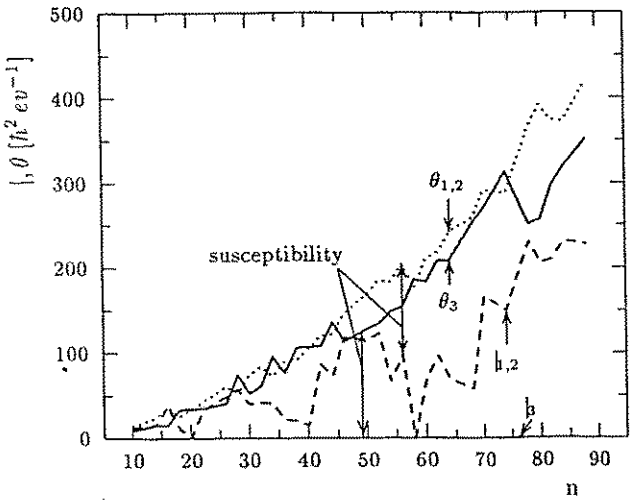

FIG. 3. Magnetic susceptibility of the valence electrons of even Na clusters calculated for the *axial* Woods Saxon potential. The susceptibility is the difference between the van Vleck term $\mathcal{J}$ and the diamagnetic term Θ.

In most even clusters the paramagnetic moments are paired off (c. f. discussion above). Only the diamagnetism remains. Maximal deflection occurs for spherical clusters, since the van Vleck term is zero. For $B = 1T$ one has

$$\left(\frac{\mu}{N}\right)_{ION} \sim 0.25 \times 10^{-4} \tag{13}$$

$$\left(\frac{\mu}{N}\right)_{VAL} \sim 0.12 \times 10^{-4} N^{2/3} \tag{14}$$

The valence electron part is 0.5×10^{-4} and 21×10^{-4} for $N = 10$ and 100, respectively. Hence, for experimental detection of the diamagnetism one would need two orders of magnitude higher sensitivity as compared to the paramagnetism.

Fig. 3 shows a calculation the magnetic susceptibility of the valence electrons, which for our choice of the units becomes a moment of inertia. It is the difference between the diamagnetic and the van Vleck term, both displayed in the figure. The calculation is done for the WS potential assuming axial shape. The largest contribution comes from the the symmetry axis 3, for which the van Vleck term is zero. For the 1- and 2- axes the van Vleck term partially compensates the diamagnetic term. The difference remains negative for all deformations, i. e. the cluster is diamgnetic. The deflection is determined by the average of the three axes. It is maximal for spherical clusters and attenuated for deformed ones.

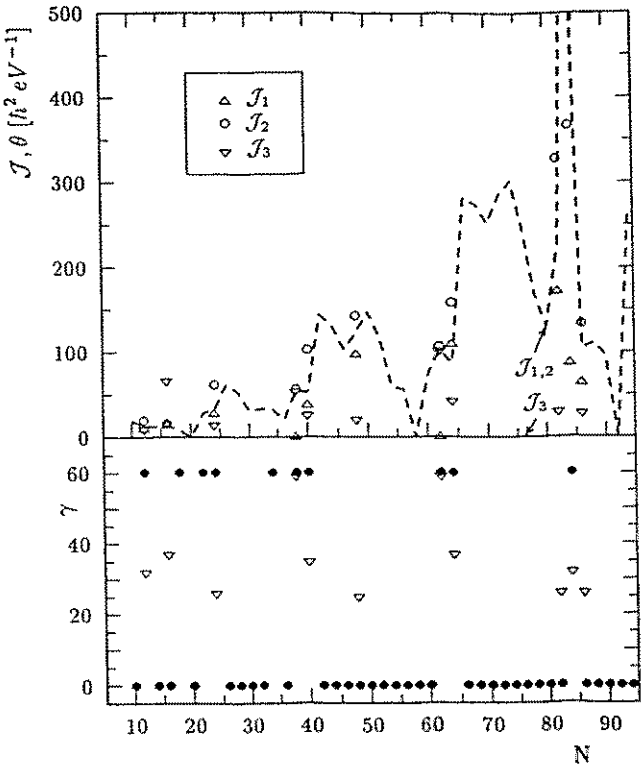

FIG. 4. Van Vleck term of the magnetic susceptibility of the valence electrons of even Na clusters calculated for the Kohn Sham Nilsson potential. The diamagnetic term Θ is expected to be similar to the one for the Woods Saxon potential. For triaxial ground states the circle and the triangles display the different values for the three axes. The lower panel shows the triaxiality parameter γ.

Fig. 4 shows a calculation of the van Vleck term for the KSN potential. The axial values are similar to the WS values. We have not calculated the diamagnetic term. It is expected to be very similar to the one for the WS potential, since it is an integral over the electron density, which is not very sensitive to the fine details of the po-

tential. For the clusters with triaxial ground states we also show the values of $\mathcal{J}_i$ for the three different axes. It is seen that the triaxiality just leads to two large values and one small value of $\mathcal{J}_i$ instead to $\mathcal{J}_1 = \mathcal{J}_2$ and $\mathcal{J}_3 = 0$ for axial shape. Triaxiality is not expected to change the deflection in a major way, since it is determined by the average over all three axes.

For N=84 we find $\mathcal{J}_1 = 86\hbar^2 eV^{-1}, \mathcal{J}_2 = 366\hbar^2 eV^{-1}$ and $\mathcal{J}_3 = 4523\hbar^2 eV^{-1}$. The large value of $\mathcal{J}_3$ is the consequence of a very low lying particle - hole excitation with a finite matrixelement of l_3, which dominates the sum (12). This is an example of van Vleck paramagnetism [3], since the term overcompensates the diamagnetic one. For $1T$ the magnetic moment is about 0.2, i. e. it reaches one tenth of the paramagnetic moments of the odd clusters. The term is strongly temperature dependent, decreasing with T.

The deflection due the diamagnetism has been estimated to increase $\propto N^{2/3}$. For large clusters this increase will taper out, since the estimate is only correct as long as the zero temperature expression (12) is still valid. The question of what happens at finite temperature has been discussed in the context of nuclear rotation [4,5]. There, the expressions for the diamagnetic and van Vleck term are called the rigid body and cranking moments of inertia. It turns out, that for sufficient high temperature the cranking moment of inertia approaches the rigid body moment. A small difference remains, which is the sum of the Landau diamagnetism and the Pauli paramagnetism of the electron gas (for the two effects c. f. [3]). Where this happens for the clusters remains to be investigated, but presumably it will occur for a temperature of $500°K$ in the mass region of several 100 atoms. This damping of the strong diamagnetism can be interpreted as an average cancellation between the persistent micro currents generating the para- and diamagnetism of the many states excited in the thermal ensemble. For clusters above 1000 the coupling of the valence electron motion to the ionic degrees of freedom begins to play a role. This is the onset of the transition from the molecular regime discussed in this paper to the macroscopic regime, where the Ohmic eddy currents, induced while entering and leaving the magnetic field, play the dominating role.

III. CALCULATION OF THE CLUSTER DEFORMATION

The cluster shapes are found by means of the shell correction method. The details are given in refs. [1,6].

Two different deformed potential are used to calculate the shell correction and to generate the electron wavefunctions entering the matrixelements of the expressions for the magnetic moments:

1) The *axial* Woods Saxon potential, which has a Fermi function profile. The shape is parametrized by the lowest five multipoles of the harmonic expansion around the sphere [1].

2) The *triaxial* Kohn Sham Nilsson potential, which consists of a spherical Kohn Sham part and a deformed harmonic oscillator part [6]. For the shape parametrization used, the difference of the three principal axes from R_o is

$$\delta R_i \propto \varepsilon_2 cos(\gamma + \frac{2\pi i}{3}), \quad i = 1,2,3 \tag{15}$$

defining the deformation parameter ε_2 and the triaxiality parameter γ. This shape is somewhat modified by a hexadecapole correction.

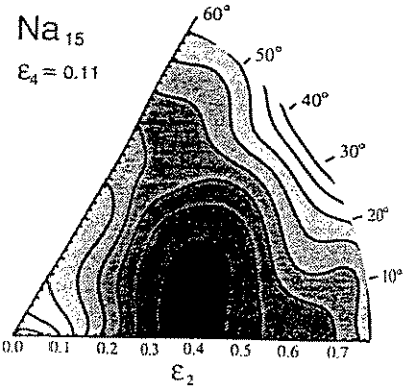

FIG. 5. The deformation energy of Na_{15} calculated for the Kohn Sham Nilsson potential. The radius gives the magnitude of the deformation ε_2 and the triaxiality parameter γ (c. f. eq.(15)). One contour line corresponds to 0.08 eV.

We have demonstrated that axial odd Na clusters with a mass below 100 are expected to show substantial orbital paramagnetism, which should be detectable by deflection of the cluster beam in a strong magnet. Triaxiality quenches the orbital paramagnetism and, thus, may serve as an experimental probe for triaxiality. The diamgnetism in even clusters is two orders of magnitude weaker. It is attenuated by deformation.

[1] S. Frauendorf, V.V. Pashkevich, Z. Phys D26 (1993) S 98; Phys. Rev. B, subm.

[2] W. de Heer, Thesis, University of California, Berkeley, 1985

[3] Ashcroft/Mermin, *Solid State Physics*

[4] V.V. Pashkevich, S. Frauendorf, Jadernaja Fisika (Soviet Nuclear Physics) 20 (1974) 1122

[5] K. Neergard, V.V. Pashkevich , S. Frauendorf Nuclear Physics A262 (1976) 61

[6] S.M. Reimann et al. Z. Phys. D28 (1993) 235 and contribution to this volume

POTENTIAL ENERGY SURFACES OF SODIUM CLUSTERS WITH QUADRUPOLE, HEXADECAPOLE AND AXIALLY ASYMMETRIC DEFORMATIONS

S.M. Reimann[a], S. Frauendorf[b]

[a] *Institut für Theoretische Physik, Universität Regensburg, D-93040 Regensburg, Germany*

[b] *Insitut für Kern- und Hadronenphysik, Forschungszentrum Rossendorf e.V., PF 510119, 01314 Dresden, Germany*

Combining a modified Nilsson-Clemenger model with the shell correction method, the potential energy surfaces of sodium clusters with sizes of up to $N = 200$ atoms are calculated, including nonaxial deformations. For spherical clusters, the model potential is fitted to the single-particle spectra obtained from microscopically selfconsistent Kohn-Sham-calculations using the jellium model and the local density approximation. Employing Strutinsky's shell correction method, the surface energy of the jellium model is renormalized to its experimental value. The ground-state shapes are determined by simultaneous minimization of the deformation energies for quadrupole, hexadecapole and triaxial cluster deformations.

K. Clemenger was the first to interpret the fine structure of sodium mass spectra [1] between the magic numbers $N = 2, 40, 58, 92...$ by *spheroidal* deformations [2]. In close analogy to the methods of nuclear physics, using a modified Nilsson Hamiltonian [3] without spin-orbit interaction he could show that it is indeed the splitting of the energy levels due to the loss of spherical symmetry, that yields stable deformed ground states. As a consequence of the Jahn-Teller effect, the subshell structure leads to enhanced cluster stabilities *between* the spherical shells predicted first by W. Ekardt in the framework of density functional theory [4]. In the meantime, cluster deformations have been extensively studied using various techniques. For clusters with $N \leq 40$, the results of Clemenger's phenomenological model have been confirmed by self-consistent calculations [5,6], which for axial deformations recently have also been extended to hexadecapole and octupole deformations [7]. Using Strutinsky's shell correction method [8], spheroidal [9,10] and general axial shapes [11] of sodium clusters have been determined for much larger cluster sizes up to $N = 800$ atoms. Using a deformed Woods-Saxon potential, a systematics of cluster deformations for simultaneous minimization of five-dimensional multipolarity is given in Ref. [11].

In the present article, we extend the spheroidal Nilsson-Clemenger model to triaxial cluster shapes. In the original model, the equilibrium state of each cluster is determined by a simple minimization of the sum over the lowest occupied single-particle energies ε_i. It is already known from nuclear physics, that the sum of the single-particle energies fails to correctly describe the deformation energy of an interacting system. Therefore, we determine the total binding energy of a cluster by use of the Strutinsky method [8] which ensures that the potential energy is not double-counted. Furthermore, the surface energy of the jellium model can be renormalized to its experimental value. The main idea of the Kohn-Sham-Nilsson model (KSN) is to construct a mean-field potential which in the spherical limit approximates the single-particle spectra of selfconsistent Kohn-Sham calculations using the jellium model and the local density approximation. Neglecting the spin-orbit term, we start from the single-particle Hamiltonian

$$H = H_{h.o.} - U \cdot \hbar\omega_0^o \hat{1}^2$$

$$\begin{aligned}\text{with} \quad H_{h.o.} = T + \frac{1}{2}\hbar\omega_0\rho^2[1 &- \frac{2}{3}\varepsilon_2\sqrt{\frac{4\pi}{5}}\cos\gamma \cdot Y_{20} + \\ &+ \frac{2}{3}\varepsilon_2\sqrt{\frac{4\pi}{5}} \cdot \frac{\sin\gamma}{\sqrt{2}}(Y_{22} + Y_{2-2}) + \\ &+ 2\varepsilon_4(\cos^2(3\gamma/2) + \frac{3}{8}\sin^2(3\gamma/2))Y_{40} - \\ &- 2\varepsilon_4\frac{\sqrt{10}}{8}\sin^2(3\gamma/2)(Y_{42} + Y_{4-2}) + \\ &+ 2\varepsilon_4\frac{\sqrt{70}}{16}\sin^2(3\gamma/2)(Y_{44} + Y_{4-4})]. \qquad (1)\end{aligned}$$

We use the strechted harmonic oscillator basis with the three frequencies

$$\omega_i = \omega_o\left(1 - \frac{2}{3}\cos(\gamma + \frac{2}{3\pi}i)\right), \qquad i = 1, 2, 3. \qquad (2)$$

The hamiltonian 1 has already been extensively used in order to study the ground state shapes, isomeric states and fission barriers barriers. Using triaxially stretched coordinates as originally proposed by Nilsson [3],

$$\chi_i = x_i \cdot \sqrt{\frac{M\omega_x}{\hbar}}, \qquad i = 1, 2, 3 \qquad (3)$$

$\rho^2 = \sum {x_i}^2$ is the radius vector in stretched coordinates. As it has been shown in the originial work by Nilsson [3] and later on for triaxial deformations by Larsson et al. [12], the strechted coordinates transform away the couplings of states between different oscillator shells, which simplifies the numerical calculations very effectively. Furthermore, as the parity $\Pi = (-1)^{N_0}$ is a good quantum number, the single-particle states of even and odd parity can be calculated separately. The condition of volume conservation is fulfilled by a scaling of ω_0. For a more detailed description of the triaxial Nilsson model we refer to [12].

The l^2–term in Eq. 1 yields an intermediate between a pure oscillator potential ($U = 0$) and a square well. It has been shown in Ref. [9], that already the simple l^2-form of the Hamiltonian reproduces the spherical spectra of selfconsistent Kohn-Sham calculations extremely well. It is therefore possible to determine the model parameter U directly from the Kohn-Sham results of Ref. [13] and to obtain a close conformity of the spherical spectrum of the Hamiltonian (1) with selfconsistent calculations. The detailed procedure is given in Ref. [9].

The overall energy scale of the potential is determined by the value of $\hbar\omega_0$. In order to adjust it to the scale of the KS spectrum, we relate it to the corresponding mean square radius. For a harmonic oscillator, the virial theorem yields

$$\hbar\omega_0 = \frac{\hbar^2(N_0 + 3/2)}{M\langle r^2\rangle}. \qquad (4)$$

We use Eq. 4 to determine $(\hbar\omega_0)^{(N_0)}$for each main shell N_0 using the weighted average $\langle r^2\rangle_{N_0}$ given by the KS calculations.

The cluster shapes are generated by the coordinates ϵ_2, ϵ_4 and γ, respectively. Hereby, ε_2 represents quadrupole–, ε_4 hexadecapole–, and γ axially asymmetric deformations. According to the nomenclature of Hill and Wheeler, $\gamma = 0°$ describes prolate and $\gamma = 60°$ oblate cluster shapes. Reflection asymmetric shapes are not studied in the present work, we refer to [11,7] for a more detailed study. Note, that the sign of ε_4 is chosen opposite to the parametrization used in Refs. [11,7] following the "Lund convention".

As usual, the renormalized deformation energies are calculated as the sum of the shell correction energy δE, and the smooth liquid drop part, for which we consider only the deformation-dependent surface correction E_{def} to the spherical drop energy

$$\triangle E_{surf} = a_s \cdot (B_{surf}(\varepsilon_2, \varepsilon_4, \gamma) - 1) \cdot N^{2/3} \qquad (5)$$

where $a_s = 0.79eV$, N is the number of atoms and B_{surf} is the ratio of the surface areas of the deformed and spherical clusters keeping the volume constant. Curvature terms are not included in the present calculations. The total deformation energy is given by

$$E_{def}(\varepsilon_2, \varepsilon_4, \gamma) = \triangle E_{surf} + \delta E(\varepsilon_2, \varepsilon_4, \gamma) \qquad (6)$$

For the calculation of the shell correction energy $\delta E(\varepsilon_2, \varepsilon_4, \gamma)$, in Strutinsky's averaging procedure we use a curvature correction polynomial of the order $2M = 6$ (cf. [14]), which fulfills the plateau condition with respect to the averaging widths γ very well. In most cases, a smoothing widths of $\gamma \approx 1.2\hbar\omega_0$ is appropriate. For the numerical diagonalisation, a sufficient number of shells $N_0 < 15$ is included in the oscillator basis, such that convergence of the shell correction energies is reached within a reasonable accuracy.

In Figure 1 we show the contours of the deformation energy surfaces of the clusters with $N = 12, 16, 86$ and 132 as an example, showing stable or meta-stable configurations of ϵ_2 and γ, respectively. The the potential energy surfaces (PES) are calculated at their hexadecapole ground state deformation ε_4 given in the diagram. For Na-12, the PES shows a single pronounced minimum at $\varepsilon_2 = 0.52, \varepsilon_4 = -0.03$ and $\gamma = 32°$. The PES of Na-16 has a minimum slightly more on the oblate side ($\varepsilon_2 = 0.48, \varepsilon_4 = 0.09, \gamma = 37°$) and shows a prolate isomer at $\varepsilon_4 = 0.68$, separated from the ground state by a barrier of approximately 0.3eV. Self-consistent calculations of nonaxial quadrupole deformations only find triaxiality for Na-12 and Na-16 [15]. The clusters Na-10, Na-14 and Na-18 have been found to be axially symmetric, which is in conformity with the KS results. The PES of quadrupole and hexadecapole deformations for axial shapes ($\gamma = 0°, 60°$) agree very nicely in a range $N \lesssim 30$ with KSN. The sphericity of Na-40, however, is not reproduced by the KSN. This is due to the KS spectrum for a steep jellium, which places the $2p$ level in the middle between the $1f$ and $1g$ levels, destroying the $N = 40$ shell gap. Below and above the critical region around 40, however, the model is in accordance with the selfconsistent and WS-calculations.

For larger clusters (Na-86 and Na-132 are shown in the lower part of Figure 1), the PES show a tendency of decreasing quadrupole deformations and show almost no metastable minima for $\varepsilon_2 \gtrsim 0.5$.

The minimized ground state deformations and shell energies are shown in Figure 2 for a size range $10 \leq N \leq 200$. Between the dominant spherical shells, strong subshell closings appear between the so-called 'magic numbers' $N = 20, (36), 58, 92, 138, 192...$ indicated in the diagram. For large clusters, similar to the results of [11], deformations on the prolate side ($\gamma \leq 30°$) predominate, and most of the axial deformations on the oblate side found in Ref. [9] become triaxial. Similar trends are known from atomic nuclei.

In summary, we have shown that stable triaxial ground states exist for sodium clusters in a size range $N < 200$. The dominant effects in deformation energies, however, come from axially symmetric quadrupole and hexadecapole effects, and triaxiality is expected to play a minor role in order to explain subshell closings in the abundance spectra. A more detailed analysis of the results, and in particular the comparison of the separation energies to the experimental cluster abundances of the Copenhagen group for $N < 400$ [16], will be given elsewhere.

We thank M. Brack and Th. Hirschmann for extensive discussions, which have been valuable contributions to this work.

[1] W.D. Knight, K. Clemenger, W.A. de Heer, W.A. Saunders, M.Y. Chou, M.L.Cohen, Phys. Rev. Lett. 52, 2141 (1984); W.D. Knight, K. Clemenger, W.A. de Heer, W.A. Saunders, Phys. rev. B31, 2539 (1985)
[2] K. Clemenger, Phys. Rev. B32, 1359 (1985)
[3] S.G. Nilsson, Mat.- Fys. Medd. Dan. Vidensk.Selsk. 29, 16 (1955)
[4] W. Ekardt, Phys. Rev. B29, 1558 (1984)
[5] W. Ekardt, Z. Penzar, Phys. Rev. B38, 4273 (1988)
[6] Th. Hirschmann, M. Brack, J. Meyer, Ann. Physik 3, 336 (1994)
[7] B. Montag, Th. Hirschmann, J. Meyer, P.-G. Reinhard, M. Brack, preprint TPR-94-19, submitted to PRL
[8] V.M. Strutinsky, Sov. J. Nucl. Phys. 3, 449 (1967), Nucl. Phys. A95, 420 (1967);*ibid.* A 122, 1 (1968)
[9] S.M. Reimann, M. Brack, K. Hansen, Z. Phys. D 28, 235 (1993)
[10] A. Bulgac, C. Lewenkopf, Phys. Rev. Lett. 71, 4130 (1993)
[11] S. Frauendorf, V. Pashkevich, Z. Phys. D26, 98 (1993); Phys. Rev. B, submitted.
[12] S.E. Larsson, et al. Nucl. Phys. A261, 77 (1976)
[13] O. Genzken, M. Brack, Phys. Rev. Lett. 67, 3286 (1991)
[14] M. Brack, H.C. Pauli, Nucl. Phys. A207, 401 (1973)
[15] G. Lauritsch, P.-G. Reinhard, M. Brack, Phys. Lett. A160, 179 (1991), M. Rotter *et al.*, to be published.
[16] S. Bjørnholm, J. Borggreen, O. Echt, K. Hansen, J. Pedersen, H. Rasmussen, Phys. Rev. Lett. 65, 1627 (1990); Z. Phys. D19, 47 (1991)
[17] S.M. Reimann, S. Frauendorf, to be published

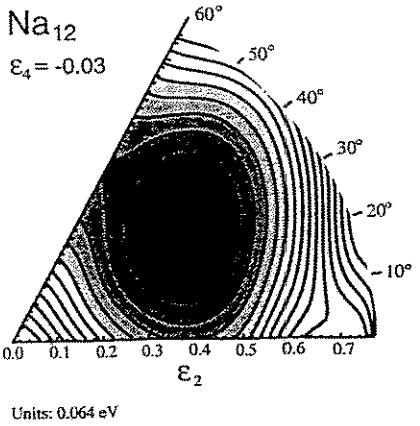

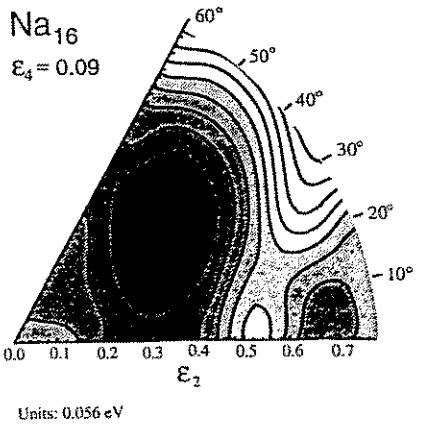

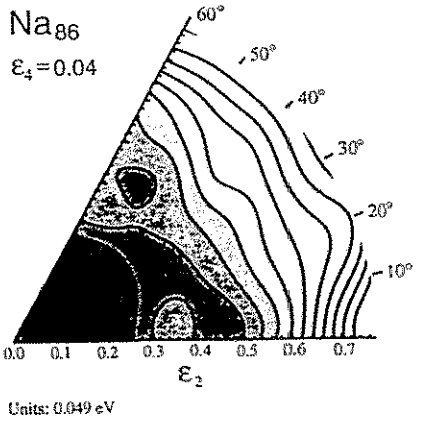

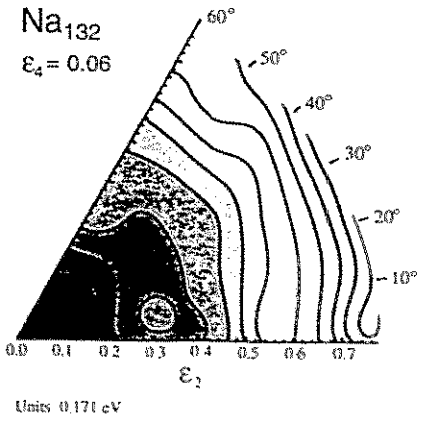

Fig. 1

Figure captions

Figure 1: Contour diagrams of the PES for $N = 12, 16, 86, 132$ for (ε_2, γ) calculated at minimized ε_4. $\gamma = 0°$ corresponds to prolate, $\gamma = 60°$ to oblate cluster shapes.

Figure 2: Shell energies and the corresponding ground state deformations $(\varepsilon_2, \varepsilon_4, \gamma)$ for $N < 200$. In the upper part, the deformation energies corresponding to one- and two-dimensional minimization of axially symmetric shapes are also shown.

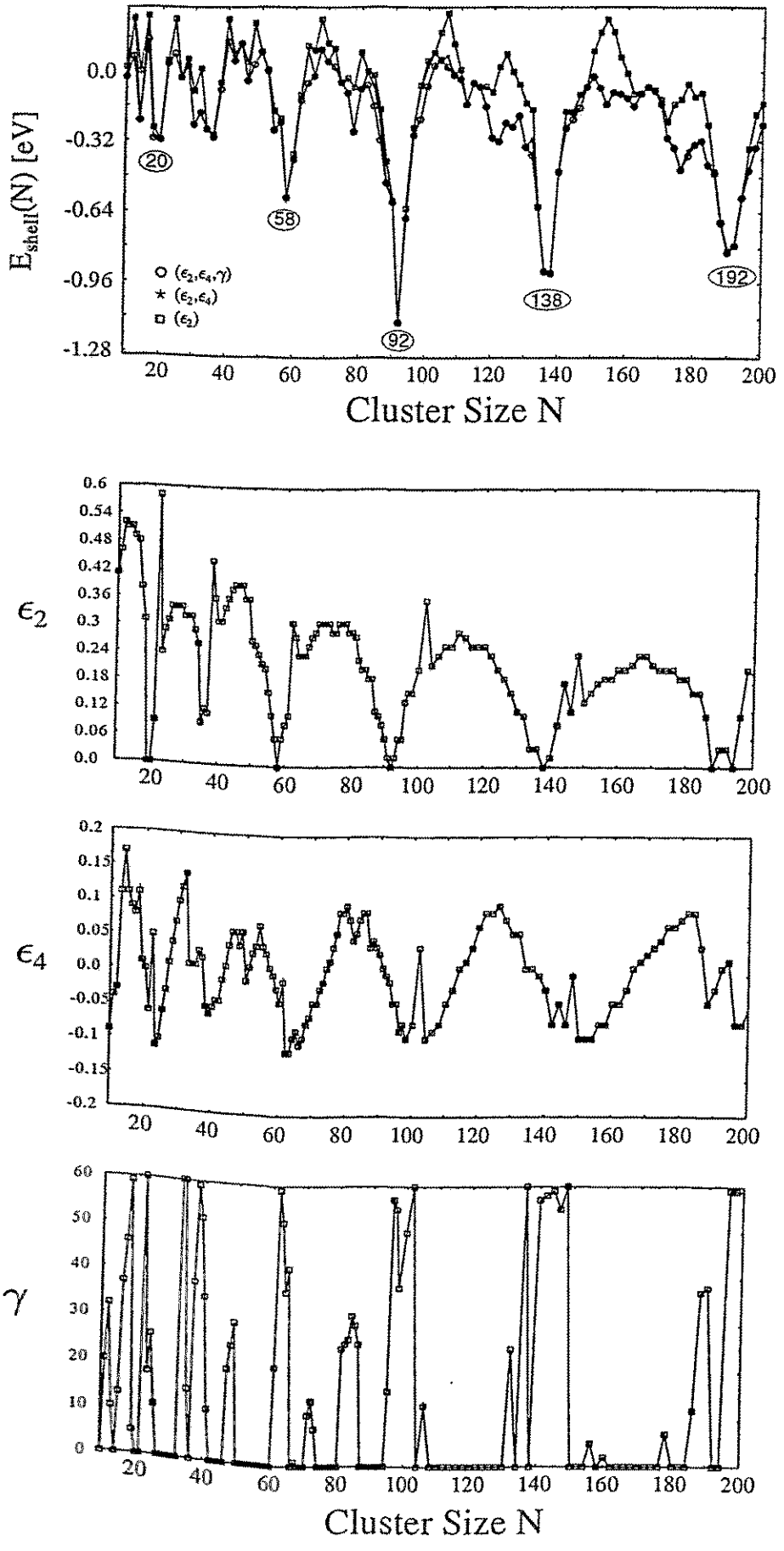
$E_{shell}(N)$ [eV]
0.0
-0.32
-0.64
-0.96
-1.28
20
58
92
138
192
○ (ϵ_2,ϵ_4,γ)
★ (ϵ_2,ϵ_4)
□ (ϵ_2)
20 40 60 80 100 120 140 160 180 200
Cluster Size N
ϵ_2
0.6 0.54 0.48 0.42 0.36 0.3 0.24 0.18 0.12 0.06 0.0
20 40 60 80 100 120 140 160 180 200
ϵ_4
0.2 0.15 0.1 0.05 0.0 -0.05 -0.1 -0.15 -0.2
20 40 60 80 100 120 140 160 180 200
γ
60 50 40 30 20 10 0
20 40 60 80 100 120 140 160 180 200
Cluster Size N

Fig.2